Accuracy in local staging of prostate cancer by adding a three-dimensional T2-weighted sequence with radial reconstructions in magnetic resonance imaging

Fredrik Jäderling[1,2], Tommy Nyberg[3], Michael Öberg[1], Stefan Carlsson[2,6], Mikael Skorpil[4,5] and Lennart Blomqvist[1,2,4]

Abstract

Background: The evidence supporting the use of magnetic resonance imaging (MRI) in prostate cancer detection has been established, but its accuracy in local staging is questioned.

Purpose: To investigate the additional value of multi-planar radial reconstructions of a three-dimensional (3D) T2-weighted (T2W) MRI sequence, intercepting the prostate capsule perpendicularly, for improving local staging of prostate cancer.

Material and Methods: Preoperative, bi-parametric prostate MRI examinations in 94 patients operated between June 2014 and January 2015 where retrospectively reviewed by two experienced abdominal radiologists. Each patient was presented in two separate sets including diffusion-weighted imaging, without and with the 3D T2W set that included radial reconstructions. Each set was read at least two months apart. Extraprostatic tumor extension (EPE) was assessed according to a 5-point grading scale. Sensitivity and specificity for EPE was calculated and presented as receiver operating characteristics (ROC) with area under the curve (AUC), using histology from whole-mount prostate specimen as gold standard. Inter-rater agreement was calculated for the two different reading modes using Cohen's kappa.

Results: The AUC for detection of EPE for Readers 1 and 2 in the two-dimensional (2D) set was 0.70 and 0.68, respectively, and for the 2D + 3D set 0.62 and 0.65, respectively. Inter-rater agreement (Reader 1 vs. Reader 2) on EPE using Cohen's kappa for the 2D and 2D + 3D set, respectively, was 0.42 and 0.17 (i.e. moderate and poor agreement, respectively).

Conclusion: The addition of 3D T2W MRI with radial reconstructions did not improve local staging in prostate cancer.

Introduction

Multi-parametric magnetic resonance imaging (mpMRI) has good detection rate of clinically significant prostate cancer (1,2), but still lacks the ability to accurately distinguish organ-confined disease from tumors growing outside the prostatic confinement (3). Correct staging is crucial for prognostic reasons (4), but even more so in a preoperative setting where the surgeon has to choose between a nerve sparing or non-nerve sparing surgical procedure. A nerve sparing procedure provides the possibility of retaining erectile

[1]Department of Radiology, Karolinska University Hospital, Solna, Sweden
[2]Department of Molecular Medicine and Surgery, Karolinska Institutet, Stockholm, Sweden
[3]Department of Oncology and Pathology, Division of Clinical Cancer Epidemiology, Karolinska Institutet, Stockholm, Sweden
[4]Department of Radiation Sciences, Umeå University, Umeå, Sweden
[5]Department of Radiology, Uppsala University Hospital, Uppsala, Sweden
[6]Department of Urology Karolinska University Hospital, Solna, Sweden

Corresponding author:
Fredrik Jäderling, Department of Radiology Karolinska University Hospital, 171 76 Stockholm, Sweden.
Email: fredrik.jaderling@ki.se

function and better prognosis regarding urinary continence, but introduces the risk of positive surgical margins in non-organ confined disease (5).

Previous studies using MRI for local staging of prostate cancer using T2-weighted (T2W) imaging have assessed direct signs such as overt capsular penetration or indirect signs such as length of tumor abutment, bulging, or irregular capsule (6–8). The use of diffusion-weighted imaging (DWI), including apparent diffusion coefficient (ADC) values, has also shown a correlation to extraprostatic tumor extension (EPE), with a higher risk at lower ADC values (9–11). Endorectal coils have been used in several studies, but a recently published meta-analysis did not show better local staging using this technique (3). Pulse sequences employed for prostate cancer staging have mainly been two-dimensional (2D) acquisitions with thinnest slice thicknesses of approximately 3 mm. One of the main reasons of the shortcoming of MRI regarding local staging is often the minute EPE, < 0.5 mm, falling out of the range of detection. Another difficulty is the relatively thick slices of 3 mm at 2D T2W imaging, giving partial volume effects at the curved portions at the base and apex of the prostate. Previous studies using three-dimensional (3D) T2W sequences with reconstructed images in the other two orthogonal planes (7,12) have shown similar results on local staging as standard T2W 2D axial imaging, 3 mm slice thickness, though the study by Cornud et al. showed better sensitivity and specificity when including indirect signs of EPE (7).

In this retrospective study, we assessed the additional value of a 3D T2W sequence with radial reconstructions with a set of images 360° around a central axis through the prostate to improve local staging. The radial reconstructions were created having its axis in the cranio-caudal direction to acquire images that all intercept the capsule perpendicularly (Fig. 1).

Material and Methods

Patients

One hundred consecutive patients who underwent robotic assisted radical prostatectomy between June
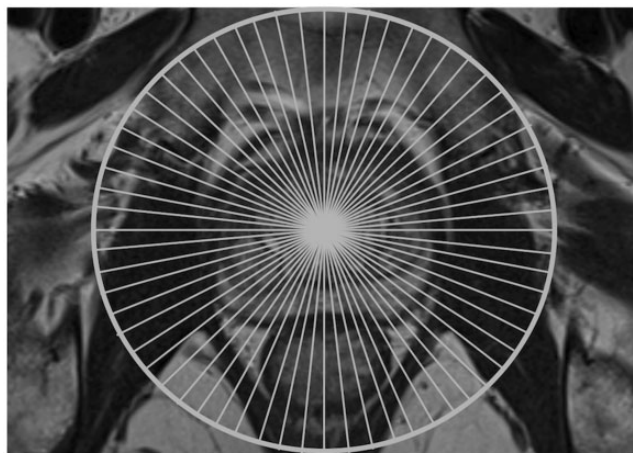

Fig. 1. Orientation of the sections for the radially reconstructed T2W 3D SPACE sequence, with 1.8° between each slice.

Table 1. Parameters for the bi-parametric magnetic resonance imaging protocol including the 3D T2W sequence.

Sequence, plane of acquisition	Pulse sequence	TR/TE	Acquired voxel size* (mm)	FOV (mm)	Slices (n)	Time of acquisition (min:s)
T2W 3D (SPACE), cor	TSE	1030/137	$0.8 \times 0.8 \times 0.7$	200×220	96	6:12
T2W 2D, sag	TSE	5020/119	$3.0 \times 0.5 \times 0.5$	200×200	35	3:52
T2W 2D, ax	TSE	3350/92	$3.0 \times 0.5 \times 0.5$	200×220	24	2:49
T1W 2D, ax	TSE	800/11	$4.0 \times 0.8 \times 0.8$	300×300	60	2:26
DWI (RESOLVE), ax b 50, 200, 1000 s/mm^2 (calculated b 1500)	Multi-shot EPI	6300/86	$4.0 \times 1.3 \times 1.3$	200×220	18	5:00

*Acquired voxel sizes are the same as voxel size displayed in the images without any reconstruction algorithm.
T2W, T2-weighted; SPACE, sampling perfection with application optimized contrasts using different flip angle evolution; T1W, T1-weighted; DWI, diffusion-weighted imaging; RESOLVE, readout segmentation of long variable echo trains; TSE, turbo spin echo; EPI, echo planar imaging; TR, repetition time; TE, echo time; FOV, field of view.

2014 and January 2015, and before surgery had a biparametric prostate MRI, were included. MRI was performed in high-risk patients (T2c–T3 and/or Gleason score 8–10 or Gleason score $4 + 3 = 7$ in > 50% of cores taken and/or PSA $\geq 20\,\mu g/L$) or to resolve uncertainties, e.g. in cases where prostate specific antigen levels were high compared to tumor grade or amount of millimeter cancer in biopsies. Six patients were excluded; one patient did not manage the complete MRI protocol, three patients due to missing information on exact tumor location in the pathology report, one patient with bilateral hip replacements and poor quality on DWI and the 3D sequence, and one patient erroneously presented with the 3D sequence at both reading sessions. This gave a final cohort of 94 patients and their characteristics are presented in Table 1. The median time between MRI and surgery was 1.7 months (interquartile range = 1–3 months).

MRI

All examinations were performed on a 3-T scanner (Magnetom Verio, Siemens Medical Systems, Erlangen, Germany) with a 32-channel phased array pelvic coil. All patients had bowel preparation using Microlax® (enema, McNeil Sweden AB, Solna, Sweden) before the examination. One milligram of Glucagon (Novo Nordisk Scandinavia AB, Malmö, Sweden) was given intramuscularly just before the examination. The protocol included sagittal and axial T2W turbo spin echo (TSE), coronal T2W 3D TSE SPACE (sampling perfection with application optimized contrasts using different flip angle evolution) with isotropic voxels $(0.8 \times 0.8 \times 0.7\,mm)$, axial DWI RESOLVE (readout segmentation of long variable echo-trains), and axial T1-weighted (T1W) TSE covering the small pelvis from the aortic bifurcation through the whole pelvis (Table 1, Suppl. 17 – full version of the protocol). No contrast enhancement or endorectal coil was used.

The reconstructions from the 3D T2W sequence were made in the scanner software with a rotation of $360°$ with $1.8°$ between each image (Fig. 1). Images were also reconstructed in the axial and sagittal plane. All reconstructions were created with a slice thickness of 0.8 mm.

MRI assessment

Two radiologists with > 20 years of experience in abdominal MRI retrospectively assessed the MRI examinations. Both radiologists assessed each patient twice and the examinations were presented in two different sets, with and without 3D T2W reconstructions as follows:

1. 2D set: (a) axial and sagittal T2W 2D; (b) coronal T2W 3D; (c) DWI with ADC map and calculated $b = 1500$ DWI images; (d) axial T1W.
2. 3D set: (a) axial and sagittal T2W 2D; (b) coronal T2W 3D with reconstructed sets of images (0.8 mm slice thickness) in: (i) axial, (ii) sagittal, (iii) radial; (c) DWI with ADC map and calculated $b = 1500$ DWI images; (d) axial T1W.

A patient presented with the reconstructed 3D image set at the first reading session was presented with the 2D set of the other reading session and vice versa. The presentation of the two different reading modes (2D or

Table 2. Characteristics of 94 patients, included in the analysis that underwent preoperative MRI before robot-assisted radical prostatectomy.

Variables (nos. missing)	Patients (n = 94)
Age (1)*	
Median	65.1
Interquartile range	61.2–69.1
Range	51.0–76.5
PSA (ng/mL) (1)	
Median	5.9
Interquartile range	4.3–9.7
Range	1.8–49.0
Biopsy Gleason (1) (%)	
≤6	9 (10)
3 + 4	46 (50)
4 + 3	19 (20)
≥8	19 (20)
Biopsy (mm) cancer (3)	
Median	18
Interquartile range	9–32
Range	1–82
Clinical T-stage (2) (%)	
T1	43 (47)
T2	36 (39)
T3	13 (14)
Postop Gleason (1) (%)	
≤6	11 (12)
3 + 4	40 (43)
4 + 3	30 (32)
≥8	12 (13)
Pathological T-stage (0) (%)	
pT2	55 (59)
pT3a (≤ 1 mm)	18 (19)
pT3a (> 1 mm or not specified)	16 (17)
pT3b	5 (5)

*One patient living abroad, lacking social security number, which includes date of birth.
PSA, prostate specific antigen.

3D) was randomly distributed for each set. The reading of each set was held at least two months apart and the patients were given random serial numbers with a different number for each patient in each set to reduce the risk of recall bias. The readers were blinded to all clinical information, only knowing that the patient was diagnosed with prostate cancer.

Tumor detection was assessed according to PI-RADS version 2 (Prostate Imaging – Reporting and Data System) and plotted into a template with the index tumor (the largest suspicious tumor area) reported as number 1 (Suppl. Fig. 1: MRI reporting template). The risk of EPE was graded 1–5. Grades 1 and 2 denote low suspicion of EPE. Grade 3 indicates risk of EPE due to tumor abutment of the capsule, but no clear sign of tumor extension beyond the prostatic confinement (13). Previously reported indirect signs as bulging, loss of or irregular capsule were graded 4 (8), and direct signs of EPE as obliteration of the recto-prostatic angle or obvious growth outside the capsule were graded 5 (14). The two readers rated image quality for the 2D T2W and 3D T2W images 1–4 (1 = poor; 2 = fair (diagnostic); 3 = good; 4 = excellent).

Surgery

Radical prostatectomy was carried out using a robot-assisted three-armed DaVinci® system (Intuitive Surgical, Sunnyvale, CA, USA).

Pathology from prostate specimen

All prostatic specimens were fixed in 10% buffered formaldehyde and subjected to whole-mount, step section according to the Stanford procedure as routine at our Pathology Department, with horizontal slicing of the specimens perpendicular to the dorsal aspect of the prostate in 3–4-mm slices. The most apical and basal slices were further cut in 3–4-mm slices in the sagittal plane (15). All slices were embedded as whole-mounts. The seminal vesicles were totally embedded. Gleason grading was carried out according to the consensus of the International Society of Urological Pathology (ISUP) 2005 (16) and evidence of extra-prostatic disease was assessed according to the ISUP consensus 2011 (17). All pathology reports were reviewed by the first author (FJ), blinded to the assessments of the two readers. The tumors were plotted into the same template as used for MRI reporting and the pathological T-stage (pT2 for organ-confined and pT3 for extraprostatic growth) for each tumor was recorded.

Data collection

Comparison of tumor location from the MRI reports for each reader and for each set (2D or 3D) was compared with the template from the pathology reports (Suppl. Fig. 2: Pathology template). Index tumor detection was catalogued either as missed, exact or approximate match. In "exact" match, the tumor was exactly

Table 3. Sensitivity, specificity, positive predictive and negative predictive value for the detection of extraprostatic tumor extension (EPE) for (a) all pT3 tumors, (b) pT3 with EPE $\leq$ 1 mm outside the prostatic capsule, (c) pT3 with EPE $>$ 1 mm outside the capsule for Readers 1 and 2 in the two different reading modes; 2D T2W and with the addition of the reconstructed 3D T2W images.

		*	Sensitivity (%)	Specificity (%)	PPV (%)	NPV (%)
2D	Reader 1	a	**77**	**48**	**56**	**70**
		b	76	48	37	83
		c	80	48	42	83
	Reader 2	a	**74**	**64**	**58**	**78**
		b	81	56	39	89
		c	72	56	39	83
3D	Reader 1	a	**77**	**43**	**53**	**69**
		b	76	51	38	85
		c	80	51	43	85
	Reader 2	a	**69**	**59**	**60**	**68**
		b	71	62	43	84
		c	68	62	45	81

*Prediction of EPE for all patients (a) and stratified on the extent of extraprostatic tumor growth (b, c).
NPV, negative predictive value (the likelihood of organ confined disease when recorded as negative for EPE at MRI compared to "gold standard" histology); PPV, positive predictive value (the likelihood of EPE being present when recorded positive for EPE at MRI when compared to "gold standard" histology).

denoted in the same position in the MRI report and in the pathology report. "Approximate" match denotes tumors located in the closest adjacent location on the MRI template compared to the pathology template, due to the known shrinkage and deformation of the prostate specimen during preparation (18,19). "Missed tumor" was registered when the location in the template from the MRI reading was not registered in an exact or an adjacent sector compared to the description in the pathology report. In some cases, the readers noted no visible tumor.

Statistical analysis

The difference in detection of extraprostatic tumor growth between the reading modes was estimated at 20%. To reach a power $(1-\beta)$ of 0.80 at a significance level of 0.05, the number of each reading mode that would be needed was calculated as 95 sets.

Index tumor detection rate for each reader and each set (2D and 3D) is presented as exact, approximate, or missed. The rate of non-visible tumors is also presented. Sensitivity and specificity for EPE for each reader and for each reading mode was calculated for each grade of
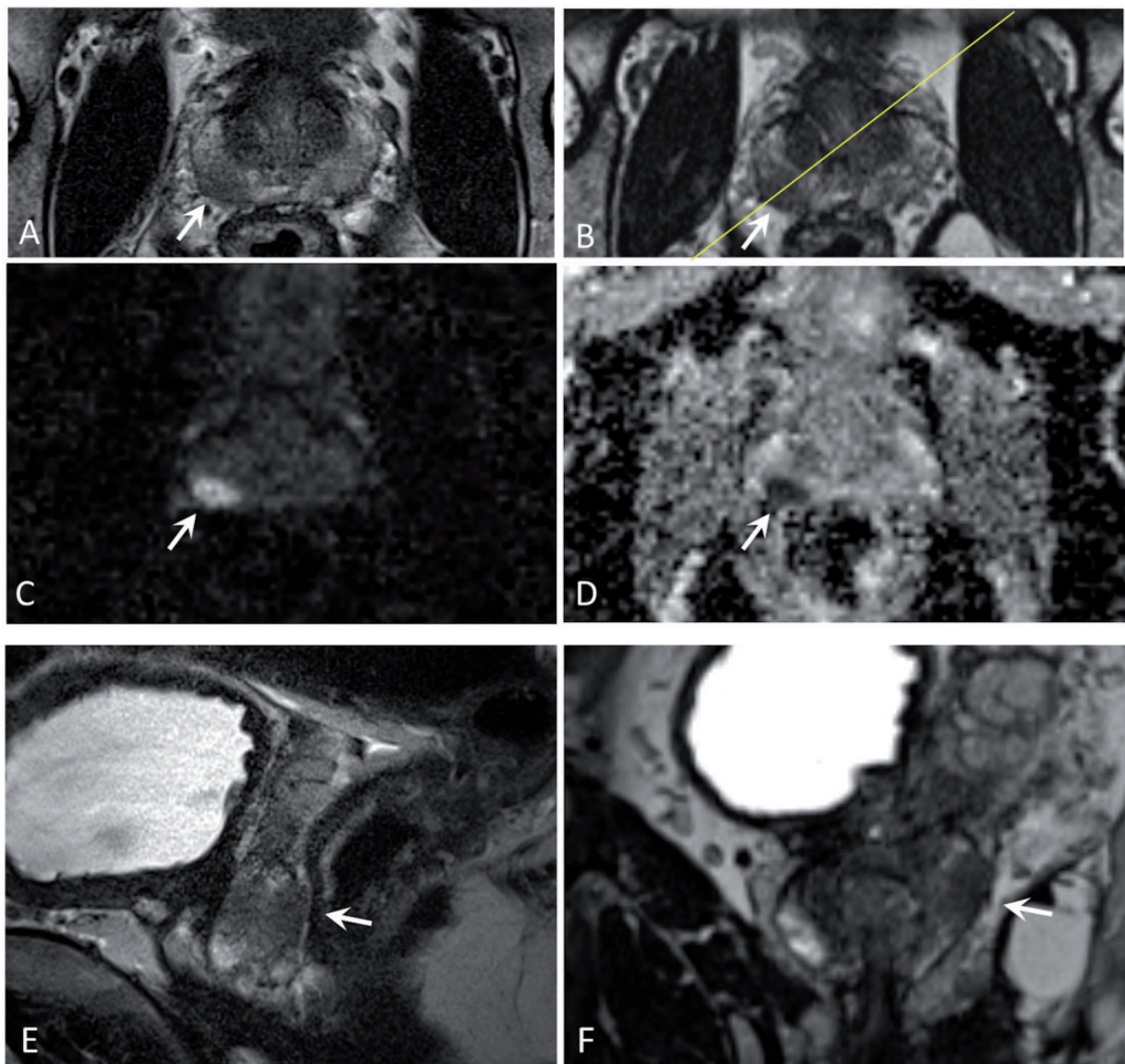

Fig. 2. (a–i) Tumor (arrows) in the peripheral zone at the base and mid-portion on the right side in axial 2D T2W image (a), axial reconstruction from T2W 3D (b), DW image calculated b = 1500 (c), ADC (d), sagittal T2W image (e), and radial reconstruction of 3D from the yellow plane of sectioning in B (f). The tumor was deemed T3 for both readers in both reading modes. Templates from histology (g), Readers 1 (h) and 2 (i) depicting tumor location with EPE assessment for each reader in bold frames. Histological outcome was Gleason $4 + 3 = 7$, pT3.
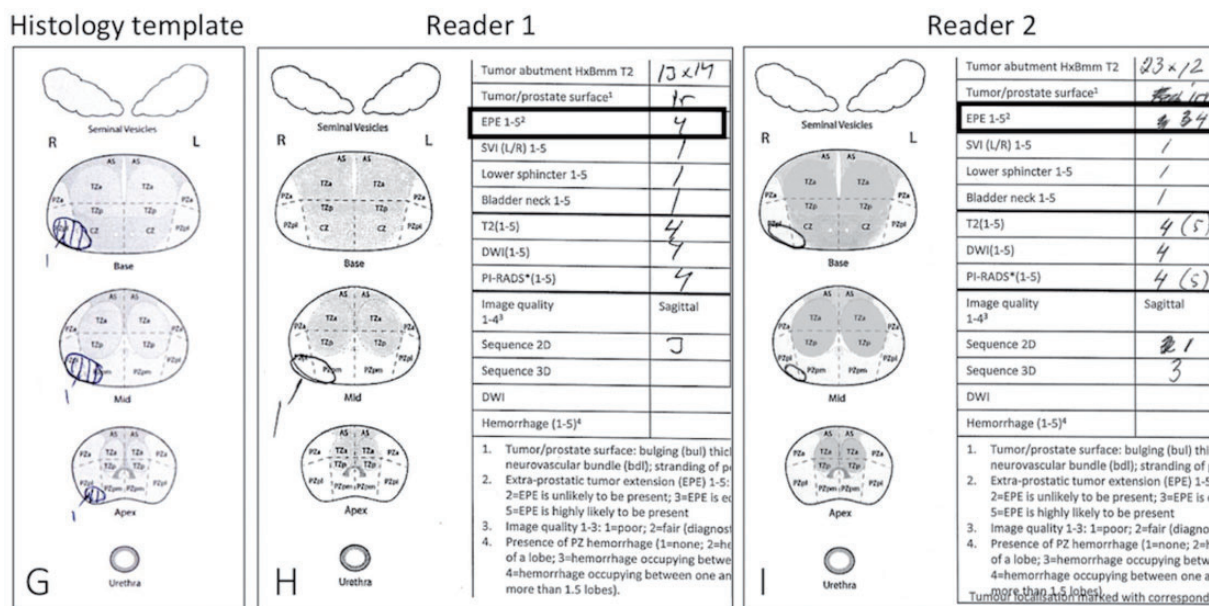
Fig. 2. Continued.

the 5-graded scale and presented as receiver operating characteristic (ROC), with area under the curve (AUC). Patients where the index tumor was missed or had no visible tumor were not part of the calculation of sensitivity and specificity for EPE. Separate sensitivity analysis for detection for EPE was performed for tumors growing ≤ 1 mm outside the capsule vs. > 1 mm outside the capsule at histology. The inter-reader agreement (Reader 1 vs. Reader 2) was calculated for the two different reading modes using Cohen's kappa (κ) interpreted as; $< 0.20 =$ poor agreement; $0.21 - 0.40 =$ fair agreement; $0.41 - 0.60 =$ moderate agreement; $0.61 - 0.80 =$ good agreement; $0.81 - 1.0 =$ very good agreement. An agreement plot was created for each reading mode. All calculations were performed using SAS software (version 9.4, SAS Institute Inc., Cary, NC, USA).

Results

Patients' characteristics are presented in Table 2. In the cohort of 94 patients, pT2 was found in 55 (59%) and pT3 in 39 (41%) at histology (Table 2). Of the pT3 tumors, 18 (19%) were at histology found to have growth ≤ 1 mm outside the capsule and 21 (22%) with > 1 mm outside the capsule.

Index tumor detection on MRI for Reader 1 with the 2D set was 80% (15% approximate match and 65% exact match) and for Reader 2 83% (16% and 67%). With the addition of the 3D reconstructions index, tumor detection for Reader 1 was 83% (15% approximate match and 68% exact match) and for Reader 2 78% (15% and 63%).

Sensitivity, specificity, positive predictive and negative predictive values when assigning grades 1–2 as an organ-confined tumor on MRI and grades 3–5 as non-organ-confined are presented in Table 3. Examples of prostate cancers from MR images and corresponding plots in the histology and reader templates are shown in Fig. 2. Additional cases are provided in Suppl. Figs. 3–16, showing disagreement between the 2D vs. 3D reading mode and between the two readers, respectively, in Suppl. Figs. 3 and 4. A variety of cases from the cohort are included in Suppl. Figs. 5–16, illustrating the difficulty in assessing correct tumor stage both at radial extraprostatic tumor extension over and under 1 mm.

The AUC for detection of EPE for Reader 1 and 2 in the 2D set was 0.70 and 0.68, respectively, and for the 3D set 0.62 and 0.65, respectively (Fig. 3).

Inter-reader agreement (Reader 1 vs. Reader 2) on EPE using Cohen's kappa (κ) for 2D and 3D set, respectively, was 0.42 and 0.17 (moderate and poor agreement, respectively) (Fig. 4).

The rating of image quality for the axial 2D T2W images was for Readers 1 and 2 3.7 (standard deviation [SD] = 0.5) and 3.7 (SD = 0.6), respectively, and for the radially reconstructed 3D 3.7 (SD = 0.5) and 3.0 (SD = 0.7), respectively.

Discussion

In this retrospective study, we investigated the additional value of reconstructing radial images, perpendicular to the prostate capsule, from a 3D T2W SPACE sequence for detection of extraprostatic tumor extension in comparison with 2D T2W imaging
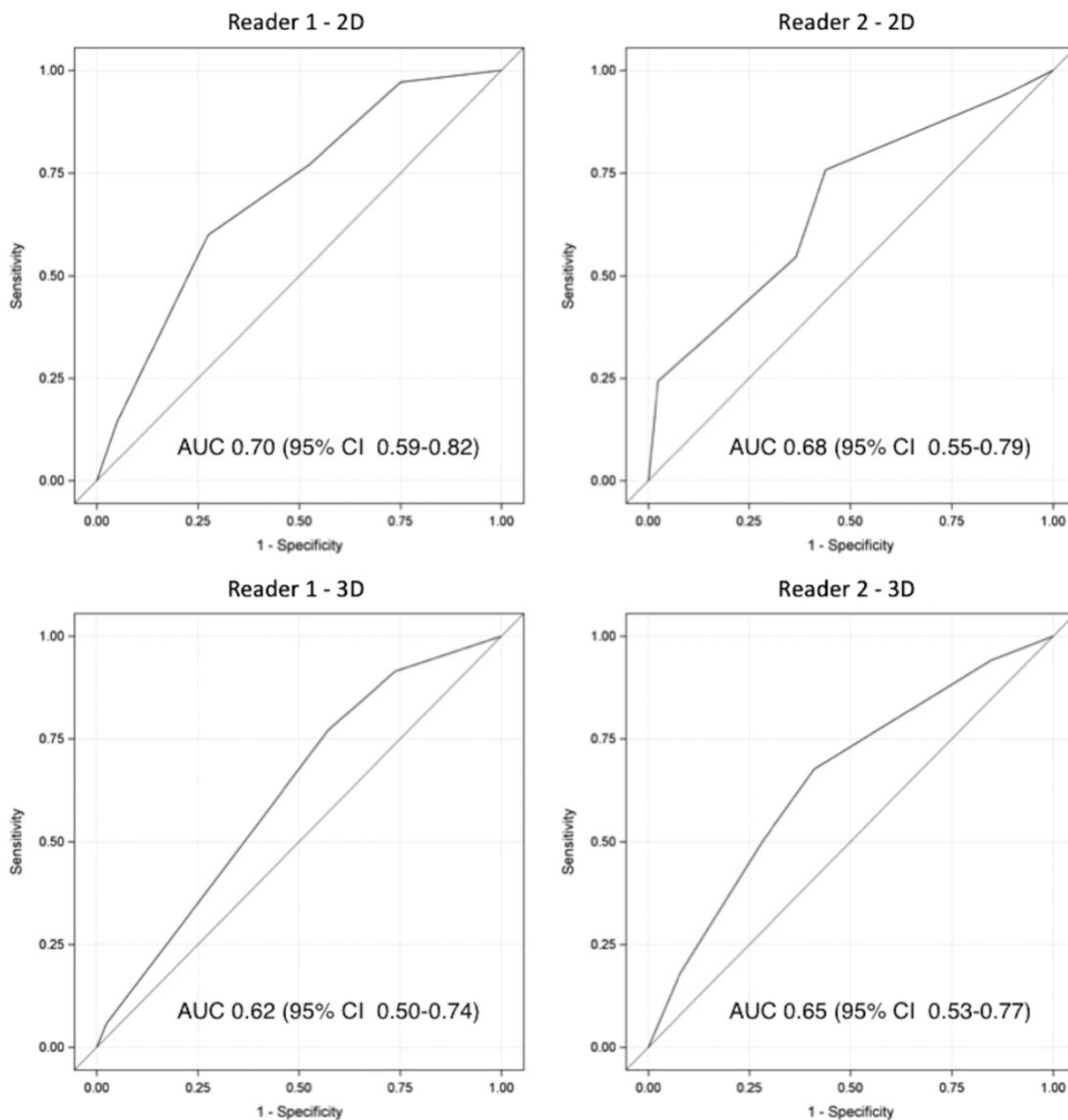
Fig. 3. AUC for detection of extraprostatic tumor extension in 2D for Reader 1 (a), for Reader 2 (b), and with the addition of 3D for Reader 1 (c) and for Reader 2 (d).

alone, finding no improvement in sensitivity or specificity.

Our index tumor detection rate was in line with a study by Le et al., where the detection rate was 80% (20). Sensitivity for EPE for both readers and with both 2D and 3D (69–77%) was higher than the pooled data in the meta-analysis by de Rooij et al. (3), having a sensitivity of 57%. However, our specificity was low (43–64%) compared to 91% in the meta-analysis by de Rooij et al., indicating that our readers had a tendency of over-staging the tumors. The AUC when using

MRI only for detection of EPE in a study by Morlacco et al. (21) was 0.70–0.71, as compared to our somewhat lower 0.62–0.70. In their study the inclusion of pre-operative nomogram by Partin and the CAPRA score (Cancer of the Prostate Risk Assessment) clearly increased the staging accuracy. Our readers did not have any clinical information at hand when assessing the MRI studies, which would facilitate prediction of EPE, e.g. a Gleason 4 + 4 that abuts the capsule has a higher probability of having EPE compared to a 3 + 4. The only information on aggressiveness that could be
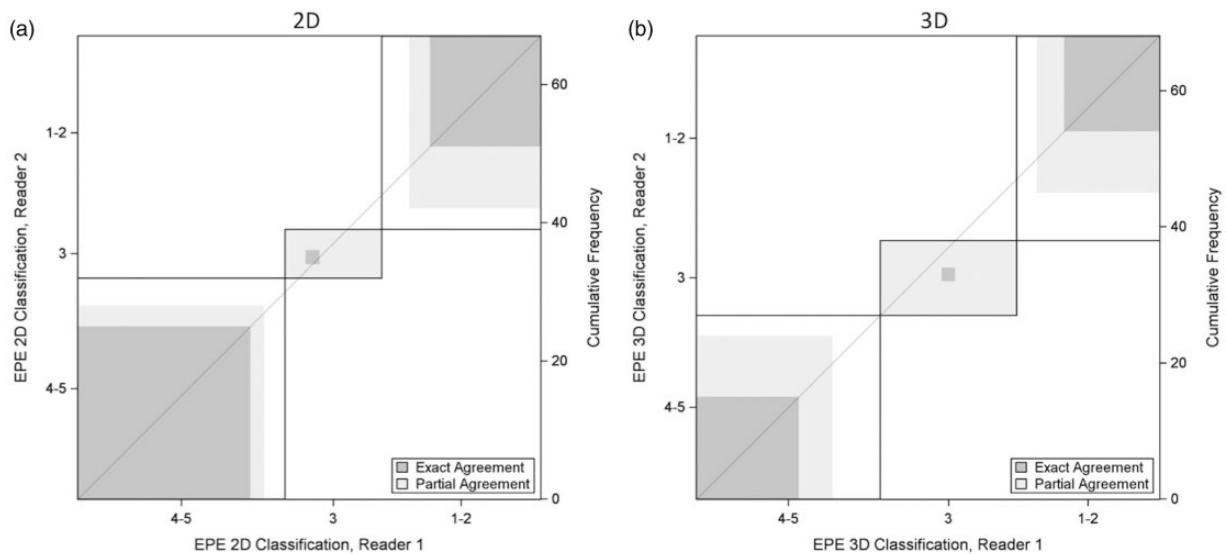
Fig. 4. Agreement plots for the two readers when assessing extraprostatic tumor extension on MRI in the 2D set (a) and the 3D set (b). The boxes denote assessment categories 1–2 (top right corner), category 3 (middle box), and categories 4–5 (bottom left corner). The exact agreement is better in 2D reading compared to 3D.

retained during the reading sessions was the ADC values (22).

Local staging of prostate cancer using MRI is challenging and requires long experience (23). In our present study the greatest difference between the reading modes 2D vs. 3D in accuracy in prediction of EPE was for Reader 1, who has immense experience in MRI reading of diseases in the small pelvis, but not specifically in prostate cancer. The 3D images seem to incorporate uncertainty in the assessment of EPE for Reader 1, with clearly a lower AUC for the 3D set. Reader 2 with longer experience in prostate MRI reading and more acquainted to the 3D sequence, showed no great difference in the assessment of EPE, but the 3D sequence did not contribute to better accuracy. An interesting finding is that Reader 1 improved his sensitivity somewhat for tumors with EPE > 1 mm compared to tumors growing ≤ 1 mm outside the capsule, which did not occur for Reader 2. Since numbers of patients are too small, no definite conclusions can be established. The concordance between the two readers was poor with the addition of 3D (Cohen's kappa $= 0.17$), which may be attributed to the lower in-plane resolution in 3D compared to 2D images, where the agreement was moderate (Cohen's kappa $= 0.42$).

Using a 3D T2W sequence with subsequent multiplanar reconstructions is appealing since just one acquisition is needed. The longer time of acquisition when aiming at higher spatial resolution approaching that of a standard 2D T2W sequence introduces the risk of movement artifacts. These artifacts always become more obvious in the reconstructed planes making the assessment of the radial reconstructions more difficult. The tendency of the 3D T2W sequence to be more prone to artifacts, from e.g. metal hip replacements, makes the sequence not suitable for all patients. The potential advantage of the radial reconstructions is that the full length of capsular abutment and bulging of the tumor can be visualized in the cranio-caudal direction at oblique angles, as indirect signs of extraprostatic tumor extension, although this could not be proven in this study.

This study does have some limitations. First, its retrospective methodology, with a somewhat limited number of patients and with only two readers resulting in uncertainties of the cause of what factor contributed the most to the outcome. It seems, though, that the lower spatial resolution is one of the main reasons for the less accurate discrimination of EPE with the 3D sequence. Second, we had to include the 3D sequence in the coronal plane when reading the 2D set, since we have omitted the standard coronal 2D T2W images from our protocol to reduce the time length of acquisition. However, since we wanted to investigate the ability of the readers to assess EPE from the radially reconstructed images primarily, this deviation was accepted from investigating a 3D set vs. a true 2D set. As a consequence of the results of this study, we presently restrict the use of the 3D sequence only for the purpose of delineating tumors for ultrasound/MRI fusion guided biopsies where the thin slices facilitates exact delineation of the tumors, but have now omitted the 3D sequence for staging purposes. There is still need for more robust techniques than currently available pulse sequences to assess minute extraprostatic disease.

In the future prediction models, including Gleason score, inherited invasiveness of the tumor by proteomics from targeted biopsies and information from MRI will probably be more accurate and robust than the current standard.

In conclusion, a 3D T2W imaging with radial reconstructions, perpendicular to the prostate capsule, does not provide additional information to a standard biparametric imaging protocol when assessing extraprostatic tumor extension in prostate cancer MRI.

Acknowledgments

Declaration of conflicting interests

Funding

Supplementary Material

Supplementary material is available for this article online.

References

1. Rud E, Klotz D, Rennesund K, et al. Detection of the index tumour and tumour volume in prostate cancer using T2-weighted and diffusion-weighted magnetic resonance imaging (MRI) alone. BJU Int 2014;114:E32–42.
2. Panebianco V, Barchetti F, Sciarra A, et al. Multiparametric magnetic resonance imaging vs. standard care in men being evaluated for prostate cancer: a randomized study. Urol Oncol 2015;33:17.
3. de Rooij M, Hamoen EH, Witjes JA, et al. Accuracy of magnetic resonance imaging for local staging of prostate cancer: a diagnostic meta-analysis. Eur Urol 2016;70: 233–245.
4. Bill-Axelson A, Holmberg L, Ruutu M, et al. Radical prostatectomy versus watchful waiting in early prostate cancer. N Engl J Med 2011;364:1708–1717.
5. Walz J, Burnett AL, Costello AJ, et al. A critical analysis of the current knowledge of surgical anatomy related to optimization of cancer control and preservation of continence and erection in candidates for radical prostatectomy. Eur Urol 2010;57:179–192.
6. Rosenkrantz AB, Shanbhogue AK, Wang A, et al. Length of capsular contact for diagnosing extraprostatic extension on prostate MRI: Assessment at an optimal threshold. J Magn Reson Imaging 2016;43:990–997.
7. Cornud F, Rouanne M, Beuvon F, et al. Endorectal 3D T2-weighted 1mm-slice thickness MRI for prostate cancer staging at 15Tesla: should we reconsider the indirects signs of extracapsular extension according to the D'Amico tumor risk criteria? Eur J Radiol 2012;81: e591–597.
8. Roethke MC, Lichy MP, Kniess M, et al. Accuracy of preoperative endorectal MRI in predicting extracapsular extension and influence on neurovascular bundle sparing in radical prostatectomy. World J Urol 2013;31: 1111–1116.
9. Lim C, Flood TA, Hakim SW, et al. Evaluation of apparent diffusion coefficient and MR volumetry as independent associative factors for extra-prostatic extension (EPE) in prostatic carcinoma. J Magn Reson Imaging 2016;43: 726–736.
10. Woo S, Cho JY, Kim SY, et al. Extracapsular extension in prostate cancer: added value of diffusion-weighted MRI in patients with equivocal findings on T2-weighted imaging. Am J Roentgenol 2015;204:W168–175.
11. Kim CK, Park SY, Park JJ, et al. Diffusion-weighted MRI as a predictor of extracapsular extension in prostate cancer. Am J Roentgenol 2014;202:W270–276.
12. Rosenkrantz AB, Neil J, Kong X, et al. Prostate cancer: Comparison of 3D T2-weighted with conventional 2D T2-weighted imaging for image quality and tumor detection. Am J Roentgenol 2010;194:446–452.
13. Outwater EK, Petersen RO, Siegelman ES, et al. Prostate carcinoma: assessment of diagnostic criteria for capsular penetration on endorectal coil MR images. Radiology 1994;193:333–339.
14. Yu KK, Hricak H, Alagappan R, et al. Detection of extracapsular extension of prostate carcinoma with endorectal and phased-array coil MR imaging: Multivariate feature analysis. Radiology 1997;202: 697–702.
15. Egevad L. Handling of radical prostatectomy specimens. Histopathology 2012;60:118–124.
16. Epstein JI, Allsbrook WC Jr, Amin MB, et al. Committee IG The 2005 International Society of Urological Pathology (ISUP) Consensus Conference on Gleason Grading of Prostatic Carcinoma. Am J Surg Pathol 2005;29:1228–1242.
17. Magi-Galluzzi C, Evans AJ, Delahunt B, et al. International Society of Urological Pathology (ISUP) Consensus Conference on Handling and Staging of Radical Prostatectomy Specimens. Working group 3: extraprostatic extension, lymphovascular invasion and locally advanced disease. Mod Pathol 2011;24:26–38.
18. Rosenkrantz AB, Deng FM, Kim S, et al. Prostate cancer: multiparametric MRI for index lesion localization–a multiple-reader study. Am J Roentgenol 2012; 199:830–837.
19. Turkbey B, Pinto PA, Mani H, et al. Prostate cancer: value of multiparametric MR imaging at 3 T for detection–histopathologic correlation. Radiology 2010;255: 89–99.

20. Le JD, Tan N, Shkolyar E, et al. Multifocality and prostate cancer detection by multiparametric magnetic resonance imaging: correlation with whole-mount histopathology. Eur Urol 2015;67:569–576.

21. Morlacco A, Sharma V, Viers BR, et al. The incremental role of magnetic resonance imaging for prostate cancer staging before radical prostatectomy. Eur Urol 2017;71: 701–704.

22. Hambrock T, Somford DM, Huisman HJ, et al. Relationship between apparent diffusion coefficients at 3.0-T MR imaging and Gleason grade in peripheral zone prostate cancer. Radiology 2011;259:453–461.

23. Ruprecht O, Weisser P, Bodelle B, et al. MRI of the prostate: interobserver agreement compared with histopathologic outcome after radical prostatectomy. Eur J Radiol 2012;81:456–460.